conditional *Lig4* and *Xrcc2* alleles that were inactivated in neural progenitor cells during development using *Nestin*-cre. We used *Xrcc2*, *Brca2* and *Lig4* mutants to compare the effects of disruption of the two mammalian DNA DSB repair pathways, NHEJ (*Lig4*) or HR (*Brca2* and *Xrcc2*). For clarity, we refer to $Lig4^{LoxP/LoxP}$;*Nestin-cre* mice as $Lig4^{Nes\text{-}Cre}$ and have used a similar nomenclature for *Xrcc2* and *Brca2* animals. While inactivation of many DNA DSB repair genes results in embryonic lethality, conditional deletion of these genes throughout the nervous system was compatible with animal survival. A notable feature of the conditional mutant animals was the lack of pronounced apoptosis typical after germline inactivation of these genes, and likely reflects developmental timing of cre expression (data not shown). However, deletion of Lig4 using Meox2-cre, which expresses in the epiblast cells, leads to similar neuraxis-wide apoptosis as germline Lig4 deletion (Lee et al., unpublished). Nestin-cre mediated deletion of the Lig4 binding protein Xrcc4 was also found to lack the neural apoptosis observed when this gene is deleted in the germline (31).

We monitored tumor formation in $Lig4^{Nes\text{-}Cre}$, $Xrcc2^{Nes\text{-}Cre}$ and $Lig4/Xrcc2^{Nes\text{-}Cre}$ mice, whereby NHEJ, HR or both repair pathways were disrupted, and for each strain we analyzed co inactivation of p53 alleles. We observed tumor formation over a period of thirty-two weeks (Fig. 1A-C). We found that $Lig4^{Nes\text{-}Cre}$, $Xrcc2^{Nes\text{-}Cre}$ and $Lig4/Xrcc2^{Nes\text{-}Cre}$ mice developed medulloblastomas between 14 and 16 weeks of age when *p53* was also inactivated (Fig. 1A-C, Table 1). Additionally, *p53* heterozygosity only promoted medulloblastomas in $(Lig4;Xrcc2)^{Nes\text{-}Cre}$ mice, compared with either DNA repair mutant alone, with a tumor onset around 22 weeks of age (Fig. 1). We determined p53 status in medulloblastoma from the $(Lig4;Xrcc2)^{Nes\text{-}Cre};p53^{+/-}$ mice. To do this we performed aCGH and real-time PCR analysis and found that the WT *p53* allele was lost (Fig.1D-E), implying that *p53* loss of heterozygosity (LOH) contributed to medulloblastoma probably reflecting increased genomic instability when both repair pathways are inactivated. For comparison to the *Lig4* and *Xrcc2*-

deficient mice, we also compared *Brca2*$^{Nes\text{-}Cre}$;*p53*$^{-/-}$ mice which also rapidly develop medulloblastoma (33), as do *Brca2*$^{Nes\text{-}cre}$;*p53*$^{+/-}$ also via inactivation of the wild type (WT) *p53* allele (Fig. 1D).

Defective DNA DSB repair leads to specific inactivation of Ptch1.

Multiple medulloblastomas from each of the different repair mutants were analyzed using aCGH and spectral karyotyping (SKY). We detected chromosome 13 alterations as a common event in medulloblastoma using aCGH, and this involved lost or translocation of one copy of chromosome 13 (Fig. 2A-C, suppl. Table 1). Analysis of the region of chr13 involved in the translocations using BAC clone assignments revealed that in all cases it involved *Ptch1*, suggesting that *Ptch1* inactivation was a key target in medulloblastoma formation. Because one copy of *Ptch1* was inactivated through chromosome loss or translocation, we determined the status of the remaining *Ptch1* allele. To do this we sequenced *Ptch1* mRNA via cDNA amplification and found mutations in the remaining *Ptch1* allele in all tumors analyzed (n=20; Fig. 2D, Suppl. Table 2). In most cases, these mutations lead to a truncated Ptch1 protein that would inactivate Ptch1 or substantially affect function. To confirm that these were *bonafide* tumor-related *Ptch1* mutations, which arose from genomic mutation, we sequenced the corresponding regions of genomic DNA. We found that in all cases genomic DNA from the tumors contained the corresponding mutation found in the cDNA. For example, splice donor/acceptor mutations were found that would predict exon skipping, as observed in the tumor-derived *Ptch1* cDNA. We also confirmed that inactivation of *Ptch1* was central to tumor formation by evaluating tumor latency and *Ptch1* status in *Ptch1*$^{+/-}$ compound mutants. We also generated *Brca2*$^{Nes\text{-}Cre}$;*Ptch1*$^{+/-}$;*p53*$^{+/-}$ (or *p53*$^{-/-}$) mice and compared tumor latency between various related genotypes (Suppl. Fig. 1). Latency was dramatically reduced (<5 weeks) in *Brca2*$^{Nes\text{-}Cre}$;*Ptch1*$^{+/-}$;*p53*$^{-/-}$ mice and aCGH or SKY

analysis of the resulting tumors showed loss of the remaining WT *Ptch1* allele, (and also *p53* in the case of *Brca2*$^{Nes\text{-}Cre}$;*Ptch1*$^{+/-}$;*p53*$^{+/-}$) (Supplementary Fig. 4). These data indicate that loss of *Ptch1* is closely linked to the genesis of medulloblastoma.

Ptch1 functions to modulate smoothened activation of Gli factor transcriptional activity (37). Consistent with Ptch1 inactivation, activation of the SHH pathway was found in all medulloblastomas analyzed (n=16; Fig. 3A). A similar gene expression profile occurred in all medulloblastomas with upregulation of a common cohort of genes, including known target genes of the Shh-signaling pathway such as *Math1*, *sFrp1*, *Ptch2*, *Gli1*, *N-Myc*, *Sox18* and *D-Cyclins*. We also confirmed the microarray expression profile using real-time PCR in comparison with wild type or *p53*$^{-/-}$ P5 and adult cerebella (Fig. 3B). Together these data indicate that inactivation of DSB repair leads to LOH of *Ptch1* and activation of the Shh pathway.

N-Myc or Cyclin D2 are amplified in the DSB repair deficient medulloblastomas

While loss of chr13/Ptch1 was a defining event in all medulloblastoma, other recurring chromosomal changes were also present. These included amplification of regions of chr12 and chr6, corresponding to *N-Myc* and *Cyclin D2*, and more selectively, loss of a portion of chr19 in medulloblastoma associated with tumors arising in Brca2 mutants or after co-inactivation of Lig4 and Xrcc2 (Fig. 4). We found that the *N-Myc* locus was amplified on chr12 (localized on two BACs: RP23-10C3 and RP23-246B9) in medulloblastoma samples spanning all DNA repair mutant genotypes (Fig. 4A, E). In some cases, N-Myc amplification was reflected by abundant double minute chromosomes; we confirmed *N-Myc* amplification in those tumors using fluorescence *in situ* hybridization (FISH) and found a strong signal corresponding to multiple copies of N-Myc (Fig. 4C).

While *N-Myc* amplification was a prominent feature in medulloblastomas, tumors not showing genomic *N-Myc* alterations were often associated with an amplification of chr6, suggesting a reciprocal relationship between N-Myc and Cyclin D2 amplification. As Cyclin D2 is expressed at high levels in the medulloblastoma and is located on Chr6, we confirmed the involvement of cyclin-D2 in many of the $Brca2^{Nes\text{-}cre};p53^{-/-}$ tumors using aCGH to map the region of chr6 that was amplified (Fig. 4A, E) and Cyclin D2 FISH (data not shown). The chromosomal changes associated with these events probably augment initial mutations acquired by the tumor, however these genes also function as SHH targets, and this fact probably accounts for enhanced expression of N-Myc and Cyclin D2 in all tumors. Thus, *Ptch1* loss and subsequent upregulation of the SHH will also promote increased N-Myc and cyclinD2 expression as seen in Fig. 3. Either *N-Myc* or *Cyclin-D2* amplification during tumor progression would contribute to the evolution of the medulloblastoma by providing a potent growth advantage.

Defective homologous recombination targets chromosome 19.

Further analysis of the genetic changes present in medulloblastomas identified a loss of chr19, by either translocation or chromosome loss associated with tumors in which HR was disabled (Fig. 4D). We found that *Brca2*-deficient (19/25), *Xrcc2*-deficient (3/9) and *Ligase4*/*Xrcc2*-deficient tumors (4/5), but not *Lig4*-deficient tumors were associated with loss of chr19; a finding consistent with the presence of a tumor suppressor gene. The loss of chromosome 19 has also been reported in some other medulloblastoma models (17, 38). Known tumor suppressors on mouse chromosome 19 include *Pten* and *Sufu*. While *SUFU* loss has been directly linked to medulloblastoma, PTEN loss has recently been associated with defective BRCA1 in breast cancer (29, 39, 40). Therefore we examined if either of these two tumor suppressors were inactivated in our medulloblastoma models. Although the *Sufu*

locus was generally associated with chr19 loss or translocation (Fig. 4E, Suppl. Table 3), sequence analysis of the remaining *Sufu* allele did not reveal mutations and *Sufu* expression was detected in all tumors suggesting that a gene(s) other than Sufu was the important target on chr19. Further, *Sufu* haploinsufficiency doesn't appear to contribute to tumorigenesis as $Sufu^{+/-}$ mice are not tumor prone, and medulloblastoma in $Sufu^{+/-}p53^{-/-}$ mice results from inactivation of the WT copy of Sufu (29).

Secondly, we determined if Pten loss was associated with the HR-deficient tumors. We sequenced *Pten* cDNA from the tumors, but did not find any exonic mutations (data not shown). However, an immunohistochemical survey of Pten expression in ten different Brca2-deficient tumor samples showed many of the tumors had lost Pten immunoreactivity (5/8) and concomitantly had increased levels of phospho-Akt (Ser473), consistent with inactivation of Pten (Fig. 5). Some tumors retained Pten expression and did not show elevated levels of p-Akt suggesting heterogeneity of expression and that Pten inactivation only occurred in a subset of tumors.

Western blot analysis of 6 Brca2-deficient tumors revealed abundant Pten signaling as Akt and S6K activity were affected in many tumors (Fig 5B). While Pten-deficient cells *in vitro* showed strong P-Akt staining, we found elevated Akt phosphorylation in some *Brca2*-deficient tumors (3/6), suggesting that the *Pten* pathway is dysfunctional in many of the tumors. It is possible that PTEN haploinsufficiency may contribute to tumorigenesis, a hypothesis that has been supported by careful studies of the effects of Pten dosage in select animal models (41). Thus, while chr19 loss is a frequent event in medulloblastoma resulting from disabled HR, the specific gene activity that is affected remains unclear, although Pten inactivation or signaling abnormalities is a feature of many HR-deficient medulloblastomas.

Discussion.

To further characterize the tumor-suppressor role of DNA DSB repair pathways in defined tissues, we used conditional inactivation of *Lig4*, *Xrcc2* and *Brca2* throughout the nervous system, and found that in conjunction with *p53* mutations, rapid development of medulloblastoma occurred. A key finding from our data is the identification of *Ptch1* as a critical target in all DNAR-deficient medulloblastomas, indicating its unique importance for preventing transformation of GNPs.

Based on microarray analysis, medulloblastomas in our study showed a gene expression profile reflective of activated SHH signaling (14). This situation reflects medulloblastoma in $Ptch1^{+/-}$ mice in which *Ptch1* LOH occurs in pre-neoplastic lesions as incipient medulloblastoma develops in $Ptch1^{+/-}$ cerebella (25). Active SHH signaling is a potent growth promoting activity, and will contribute significantly to growth and expansion of GNP cells. Initial loss of a *Ptch1* allele may promote enhanced proliferation via mild mitigation of smoothened inhibition of Shh signaling, leading to an increase in replication stress such as premature termination, replication fork collapse and generation of DNA double strand breaks (42). Subsequently, defective DNA damage responses in the mutant mice will sustain increased DNA damage leading to oncogenic mutations (such as N-Myc/CyclinD2 amplification; see below) that overcome senescence and result in transformation (43-47).

Together with *Ptch1* inactivation, we also observed *N-Myc* or *CyclinD2* amplification in medulloblastomas, both of which are Gli targets. N-Myc is critical for GNP proliferation (48-50), while the D-cyclins influence cerebellar development and GNP proliferation (51-54). Thus, loss of Ptch1 function will lead to a Gli-dependent transcriptional upregulation of N-Myc and CyclinD2. Despite increased expression of N-Myc as a result of Ptch1 loss and activated SHH signaling we also found genomic amplification of *N-Myc* and *CyclinD2* in the medulloblastomas. N-Myc amplification was also found in medulloblastomas arising after

neural inactivation of *Xrcc4* (31). We also found a mutual exclusivity between N-Myc and Cyclin D2 genomic amplification suggesting, that in addition to increased Shh target expression, there is a significant advantage to a tumor cell for additional upregulation of the growth promoting factors. The tumorigenic properties of Myc have recently been linked to a function during DNA replication via interactions with minichromosome maintenance (MCM) subunits to participate in the control of DNA replication origin activity (55). Therefore, increased expression of N-Myc may lead to increased replication firing and associated DNA damage and checkpoint activation (55), generating a compounding scenario in DNAR-deficient GNPs that significantly promotes oncogenic mutation accumulation.

Finally, we observed genomic rearrangements of chromosome 19 in tumors resulting from HR disruption. The consistent loss of chromosome 19 among tumors suggests that this chromosome contains a tumor suppressor gene whose loss contributes to medulloblastoma formation. Two well-described tumor suppressors reside on this chromosome; *Sufu* and *Pten*. *Sufu* is mutated in a subset of human medulloblastomas (40) while *Pten* is responsible for Lhermitte-Duclos disease and is mutated in some gliomas (56, 57). PTEN has recently been found as a target for mutation in breast cancer when HR is disrupted, and Pten can modulate growth in animal models of medulloblastoma (39, 58). We surveyed Pten expression in Brca2-null tumors and found that a subset of the tumors had lost Pten immunoreactivity and showed a concomitant increase in phospho-Akt (Ser473). Despite this, some tumors retained PTEN expression although phospho-Akt was still increased. In these cases it is possible that PTEN haploinsufficiency may contribute to tumorigenesis, a hypothesis that has been supported by careful studies of the effects of Pten dosage in select animal models (41).

It is likely that defective DNA DSB repair generates a continuum of genomic alterations during cell proliferation that allow for uncoupling of the growth controls of the GNPs. The genomic changes reflect the specific minimal changes that are required to

transform granule neurons in vivo, providing the blueprint for GNP transformation. Generating other brain tumor types using the approaches described above will be particularly valuable in assessing important genetic changes that underpin other tumor types. For example, combined Brca2 loss and p53 haploinsufficiency can delay or bypass medulloblastoma resulting in gliomas (Frappart et al, unpublished observation). Given the relatively homogenous nature of these tumor models, they will provide important data regarding genomic changes that lead to tumorigenesis and will also be important tools for pre-clinical studies.

Acknowledgements

We thank the Hartwell Center, the Cancer Center Cytogenetics Core and the Transgenic Core facility at SJCRH for their support of this work. These studies were supported by the NIH (NS-37956 and CA-21765) and the CCSG, (P30 CA21765) and the American Lebanese and Syrian Associated Charities (ALSAC) of St. Jude Children's Research Hospital.

Materials and methods.

Generation of Brca2$^{Nes\text{-}Cre}$, Xrcc2$^{Nes\text{-}Cre}$, Ligase4$^{Nes\text{-}Cre}$, p53-deficient mice

Brca2$^{Nes\text{-}Cre}$ and *Xrcc2*$^{Nes\text{-}Cre}$ were generated as described previously (9, 30, 33) and crossed with *p53*$^{+/-}$ mice in order to obtain the various groups used in this study. The conditional Lig4 mouse contains LoxP sites surrounding the single *Lig4* coding exon and was generated by standard methods. Tumor formation was monitored over a period of eight months.

SKY and array CGH analysis

Genomic DNA was prepared from brain tumors using the DNeasy® blood and tissue kit (QIAGEN), and metaphase spreads were from tumors after injection of colcemid (33). SKY and array CGH analysis were performed as described previously (24).

Microarrays analysis

Isolation of RNA, synthesis of cDNA, GeneChip Hybridization and Data analysis were performed as described previously (14, 16).

Real-Time RT-PCR

The *Ptch1*, *Ptch2*, *Gli1*, *Math1* and *Sufu* primer/probe sets for realtime PCR and the procedures have been described (24, 29). The primer/probe set for Titest was forward primer (5'GCGTGGTCAGGGACGAGTT), reverse primer (5' CCATCAGACAGCGGGATAAGA) and TaqMan probe (5' TCTCTGTCGGCCTTGACTCAGCCC).

Sequence analysis of candidate genes.

The cDNA was synthesized as described (24, 29). The primers Ptch1-14 (5'-ACGCGCAATGTGGCAATGGAAGGC-3') and Ptch1-R1 (5'-GAAGCGGCCGCTTCAGATTTTAATTACCC-3') were used to amplify the full length Ptch1 in a first round. Then a second round of PCR was done to amplify five overlapping fragments covering the entire length. Fragment A : Ptch1-F (5'-ATGGCCTCGGCTGGTAACG-3') / Ptch1-1 (5'-AAGGCCGGTCCATGTACCCATGGC-3'); fragment B : Ptch1-2 (5'-GCTTAATCATTACACCTTTGGACTGC-3') / Ptch1-6 (5'-AAAGGAGCATAGTGCTTCTCTGC-3'); fragment C: Ptch1-5 (5'-TTGAGCCACAGGCCTACACAGAGC-3')/Ptch1-8 (5'-GTCTGAGGTGTCTCGTAGGCCG-3'); fragment D : Ptch1-7 (5'-TGGGAAACTGGGAGGATCATGC-3') / Ptch1-10 (5'-GCTCAGGCGAAGGAGTGGGCAGTCG-3'); fragment E : Ptch1-9 (5'-GTGGAGTTCACCGTCCACGTGGC-3')/ Ptch1-R2 (5'-GAAGCGGCCGCTCAGTTGGAGCTGCTCCCCCACGGC-3'). The PCR products were sequenced. Nevertheless, if several PCR products were found, they were cloned into pGEM-T easy vector (Promega) and sequenced. The primers used to amplify full length *Sufu* in a first round PCR were: SUFU-F (5'-CTCTACCCTCCCGGGTTCTCCGC -3') and SUFU-R (5'-CCCTGCAGGGCACAGCCCAGGC -3'). Sufu sequencing was done using the same primers, plus two additional internal primers SUFU3 (5'-GCGGGGAGAAACCATATTTGAGATCG-3') and SUFU4 (5'-CTCCGGCTATCCTCTTCATCCTCCG-3').

Immunohistochemistry and Western blots.

Tissue was disrupted in lysis solution (50mM Tris, 200mM Nacl, 1% Tween 20, 0.2% NP40, 2mM PMSF, 50mM B-glycerol phosphate, pH=7.5) for four hours. Proteins were then separated on 4-12% NuPage Bis-tris gels (Invitrogen) with MOPS buffer, and transferred to

nitrocellulose (Biorad). Antibodies used were; phospho ser473-AKT (1/500, Cell Signaling, #9271), phospho ser235/236-S6 ribosomal (1/500, Cell Signaling, #2211) and PTEN (1/1000, Cell Signaling, #9559).

Table 1. Medulloblastoma incidence in mice with defective DNA DSB repair.

Genotype	Affected/total animals	Incidence	Onset (weeks) ± SD
$Lig4^{Nes\text{-}Cre}$	0/42	0%	-
$Lig4^{Nes\text{-}Cre}$, $p53^{+/-}$	0/19	0%	-
$Lig4^{Nes\text{-}Cre}$, $p53^{-/-}$	17/18	94%	16.4 ± 3.67
$Xrcc2^{Nes\text{-}Cre}$	0/23	0%	-
$Xrcc2^{Nes\text{-}Cre}$, $p53^{+/-}$	0/10	0%	-
$Xrcc2^{Nes\text{-}Cre}$, $p53^{-/-}$	28/28	100%	15.6 ± 3.12
$Lig4^{Nes\text{-}Cre}$,$Xrcc2^{Nes\text{-}Cre}$	0/25	0%	-
Lig4,$Xrcc2^{Nes\text{-}Cre}$, $p53^{+/-}$	6/8	75%	22.5 ± 2.35
Lig4,$Xrcc2^{Nes\text{-}Cre}$, $p53^{-/-}$	3/3	100%	14 ± 1.41
$Brca2^{Nes\text{-}Cre}$	0/31	0%	-
$Brca2^{Nes\text{-}Cre}$, $p53^{+/-}$	34/47	72%	20.53 ± 5.64
$Brca2^{Nes\text{-}Cre}$, $p53^{-/-}$	19/22	87%	13.26 ± 2.86

References.

1. West, S. C. (2003) *Nat Rev Mol Cell Biol* **4,** 435-445.
2. Wyman, C., Ristic, D., & Kanaar, R. (2004) *DNA Repair (Amst)* **3,** 827-833.
3. Lomonosov, M., Anand, S., Sangrithi, M., Davies, R., & Venkitaraman, A. R. (2003) *Genes & development* **17,** 3017-3022.
4. Thacker, J. & Zdzienicka, M. Z. (2004) *DNA Repair (Amst)* **3,** 1081-1090.
5. Bassing, C. H. & Alt, F. W. (2004) *DNA Repair (Amst)* **3,** 781-796.
6. Lieber, M. R., Ma, Y., Pannicke, U., & Schwarz, K. (2003) *Nat Rev Mol Cell Biol* **4,** 712-720.
7. van Gent, D. C. & van der Burg, M. (2007) *Oncogene* **26,** 7731-7740.
8. Wyman, C. & Kanaar, R. (2006) *Annual review of genetics* **40,** 363-383.
9. Orii, K. E., Lee, Y., Kondo, N., & McKinnon, P. J. (2006) *Proceedings of the National Academy of Sciences of the United States of America* **103,** 10017-10022.
10. Lee, Y. & McKinnon, P. J. (2007) *Neuroscience* **145,** 1365-1374.
11. Gilbertson, R. J. & Ellison, D. W. (2007) *Annu Rev Pathol.*
12. Wechsler-Reya, R. & Scott, M. P. (2001) *Annual review of neuroscience* **24,** 385-428.
13. Kho, A. T., Zhao, Q., Cai, Z., Butte, A. J., Kim, J. Y., Pomeroy, S. L., Rowitch, D. H., & Kohane, I. S. (2004) *Genes & development* **18,** 629-640.
14. Lee, Y., Miller, H. L., Jensen, P., Hernan, R., Connelly, M., Wetmore, C., Zindy, F., Roussel, M. F., Curran, T., Gilbertson, R. J., *et al.* (2003) *Cancer research* **63,** 5428-5437.
15. Tong, W. M., Ohgaki, H., Huang, H., Granier, C., Kleihues, P., & Wang, Z. Q. (2003) *Am J Pathol* **162,** 343-352.
16. Uziel, T., Zindy, F., Xie, S., Lee, Y., Forget, A., Magdaleno, S., Rehg, J. E., Calabrese, C., Solecki, D., Eberhart, C. G., *et al.* (2005) *Genes & development* **19,** 2656-2667.
17. Zindy, F., Uziel, T., Ayrault, O., Calabrese, C., Valentine, M., Rehg, J. E., Gilbertson, R. J., Sherr, C. J., & Roussel, M. F. (2007) *Cancer research* **67,** 2676-2684.
18. Bakhshi, S., Cerosaletti, K. M., Concannon, P., Bawle, E. V., Fontanesi, J., Gatti, R. A., & Bhambhani, K. (2003) *J Pediatr Hematol Oncol* **25,** 248-251.
19. Offit, K., Levran, O., Mullaney, B., Mah, K., Nafa, K., Batish, S. D., Diotti, R., Schneider, H., Deffenbaugh, A., Scholl, T., *et al.* (2003) *J Natl Cancer Inst* **95,** 1548-1551.

20. Dellovade, T., Romer, J. T., Curran, T., & Rubin, L. L. (2006) *Annual review of neuroscience* **29,** 539-563.
21. Giordana, M. T., Duo, D., Gasverde, S., Trevisan, E., Boghi, A., Morra, I., Pradotto, L., Mauro, A., & Chio, A. (2002) *Neuro-oncol* **4,** 115-122.
22. Woodburn, R. T., Azzarelli, B., Montebello, J. F., & Goss, I. E. (2001) *J Neurooncol* **52,** 57-62.
23. Goodrich, L. V., Milenkovic, L., Higgins, K. M., & Scott, M. P. (1997) *Science* **277,** 1109-1113.
24. Lee, Y., Miller, H. L., Russell, H. R., Boyd, K., Curran, T., & McKinnon, P. J. (2006) *Cancer research* **66,** 6964-6971.
25. Oliver, T. G., Read, T. A., Kessler, J. D., Mehmeti, A., Wells, J. F., Huynh, T. T., Lin, S. M., & Wechsler-Reya, R. J. (2005) *Development (Cambridge, England)* **132,** 2425-2439.
26. Wetmore, C., Eberhart, D. E., & Curran, T. (2001) *Cancer research* **61,** 513-516.
27. Jacks, T., Remington, L., Williams, B. O., Schmitt, E. M., Halachmi, S., Bronson, R. T., & Weinberg, R. A. (1994) *Curr Biol* **4,** 1-7.
28. Marino, S. (2005) *Trends Mol Med* **11,** 17-22.
29. Lee, Y., Kawagoe, R., Sasai, K., Li, Y., Russell, H. R., Curran, T., & McKinnon, P. J. (2007) *Oncogene*.
30. Lee, Y. & McKinnon, P. J. (2002) *Cancer research* **62,** 6395-6399.
31. Yan, C. T., Kaushal, D., Murphy, M., Zhang, Y., Datta, A., Chen, C., Monroe, B., Mostoslavsky, G., Coakley, K., Gao, Y., *et al.* (2006) *Proceedings of the National Academy of Sciences of the United States of America* **103,** 7378-7383.
32. Pazzaglia, S., Mancuso, M., Atkinson, M. J., Tanori, M., Rebessi, S., Majo, V. D., Covelli, V., Hahn, H., & Saran, A. (2002) *Oncogene* **21,** 7580-7584.
33. Frappart, P. O., Lee, Y., Lamont, J., & McKinnon, P. J. (2007) *Embo J* **26,** 2732-2742.
34. Holcomb, V. B., Vogel, H., Marple, T., Kornegay, R. W., & Hasty, P. (2006) *Oncogene* **25,** 7159-7165.
35. Frank, K. M., Sharpless, N. E., Gao, Y., Sekiguchi, J. M., Ferguson, D. O., Zhu, C., Manis, J. P., Horner, J., DePinho, R. A., & Alt, F. W. (2000) *Mol Cell* **5,** 993–1002.
36. Gao, Y., Ferguson, D. O., Xie, W., Manis, J. P., Sekiguchi, J., Frank, K. M., Chaudhuri, J., Horner, J., DePinho, R. A., & Alt, F. W. (2000) *Nature* **404,** 897-900.
37. Lum, L. & Beachy, P. A. (2004) *Science* **304,** 1755-1759.

38. Shakhova, O., Leung, C., van Montfort, E., Berns, A., & Marino, S. (2006) *Cancer research* **66,** 5190-5200.

39. Saal, L. H., Gruvberger-Saal, S. K., Persson, C., Lovgren, K., Jumppanen, M., Staaf, J., Jonsson, G., Pires, M. M., Maurer, M., Holm, K., *et al.* (2008) *Nature genetics* **40,** 102-107.

40. Taylor, M. D., Liu, L., Raffel, C., Hui, C. C., Mainprize, T. G., Zhang, X., Agatep, R., Chiappa, S., Gao, L., Lowrance, A., *et al.* (2002) *Nature genetics* **31,** 306-310.

41. Chen, Z., Trotman, L. C., Shaffer, D., Lin, H. K., Dotan, Z. A., Niki, M., Koutcher, J. A., Scher, H. I., Ludwig, T., Gerald, W., *et al.* (2005) *Nature* **436,** 725-730.

42. Branzei, D. & Foiani, M. (2005) *Curr Opin Cell Biol* **17,** 568-575.

43. Bartkova, J., Horejsi, Z., Koed, K., Kramer, A., Tort, F., Zieger, K., Guldberg, P., Sehested, M., Nesland, J. M., Lukas, C., *et al.* (2005) *Nature* **434,** 864-870.

44. Bartkova, J., Rezaei, N., Liontos, M., Karakaidos, P., Kletsas, D., Issaeva, N., Vassiliou, L. V., Kolettas, E., Niforou, K., Zoumpourlis, V. C., *et al.* (2006) *Nature* **444,** 633-637.

45. Braig, M., Lee, S., Loddenkemper, C., Rudolph, C., Peters, A. H., Schlegelberger, B., Stein, H., Dorken, B., Jenuwein, T., & Schmitt, C. A. (2005) *Nature* **436,** 660-665.

46. Di Micco, R., Fumagalli, M., Cicalese, A., Piccinin, S., Gasparini, P., Luise, C., Schurra, C., Garre, M., Nuciforo, P. G., Bensimon, A., *et al.* (2006) *Nature* **444,** 638-642.

47. Gorgoulis, V. G., Vassiliou, L. V., Karakaidos, P., Zacharatos, P., Kotsinas, A., Liloglou, T., Venere, M., Ditullio, R. A., Jr., Kastrinakis, N. G., Levy, B., *et al.* (2005) *Nature* **434,** 907-913.

48. Hatton, B. A., Knoepfler, P. S., Kenney, A. M., Rowitch, D. H., de Alboran, I. M., Olson, J. M., & Eisenman, R. N. (2006) *Cancer research* **66,** 8655-8661.

49. Kenney, A. M., Cole, M. D., & Rowitch, D. H. (2003) *Development (Cambridge, England)* **130,** 15-28.

50. Oliver, T. G., Grasfeder, L. L., Carroll, A. L., Kaiser, C., Gillingham, C. L., Lin, S. M., Wickramasinghe, R., Scott, M. P., & Wechsler-Reya, R. J. (2003) *Proceedings of the National Academy of Sciences of the United States of America* **100,** 7331-7336.

51. Ciemerych, M. A., Kenney, A. M., Sicinska, E., Kalaszczynska, I., Bronson, R. T., Rowitch, D. H., Gardner, H., & Sicinski, P. (2002) *Genes & development* **16,** 3277-3289.

52. Huard, J. M., Forster, C. C., Carter, M. L., Sicinski, P., & Ross, M. E. (1999) *Development (Cambridge, England)* **126,** 1927-1935.

53. Pogoriler, J., Millen, K., Utset, M., & Du, W. (2006) *Development (Cambridge, England)* **133,** 3929-3937.

54. Zindy, F., Knoepfler, P. S., Xie, S., Sherr, C. J., Eisenman, R. N., & Roussel, M. F. (2006) *Proceedings of the National Academy of Sciences of the United States of America* **103,** 11579-11583.

55. Dominguez-Sola, D., Ying, C. Y., Grandori, C., Ruggiero, L., Chen, B., Li, M., Galloway, D. A., Gu, W., Gautier, J., & Dalla-Favera, R. (2007) *Nature* **448,** 445-451.

56. Baker, S. J. & McKinnon, P. J. (2004) *Nat Rev Cancer* **4,** 184-196.

57. Chow, L. M. & Baker, S. J. (2006) *Cancer letters* **241,** 184-196.

58. Hambardzumyan, D., Becher, O. J., Rosenblum, M. K., Pandolfi, P. P., Manova-Todorova, K., & Holland, E. C. (2008) *Genes & development* **22,** 436-448.

Figure Legends.

Figure 1: *p53* deficiency induces medulloblastomas formation in *Lig4*$^{Nes\text{-}Cre}$ and *Xrcc2*$^{Nes\text{-}Cre}$ mice. (A) Survival curves of *Lig4/p53* deficient mice. *Lig4*$^{Nes\text{-}Cre}$ (n=42), *Lig4*$^{Nes\text{-}Cre}$, *p53*$^{+/-}$ (n=19) and *Lig4*$^{Nes\text{-}Cre}$, *p53*$^{-/-}$ (n=23) mice, were monitored over a period of 32 weeks for survival and medulloblastoma development. The life span of *Lig4*$^{Nes\text{-}Cre}$,*p53*$^{-/-}$ mice was significantly shorter compared with the *Lig4*$^{Nes\text{-}Cre}$, and *Lig4*$^{Nes\text{-}Cre}$, *p53*$^{+/-}$ cohort ($p<0.0001$). (B) Survival curves of *Xrcc2/p53* deficient mice. *Xrcc2*$^{Nes\text{-}Cre}$ (n=23), *Xrcc2*$^{Nes\text{-}Cre}$, *p53*$^{+/-}$ (n=11), *Xrcc2*$^{Nes\text{-}Cre}$, *p53*$^{-/-}$ (n=33). The life span of *Xrcc2*$^{Nes\text{-}Cre}$, *p53*$^{-/-}$ mice was significantly shorter compared with the *Xrcc2*$^{Nes\text{-}Cre}$, *p53*$^{+/-}$ and *Xrcc2*$^{Nes\text{-}Cre}$ ($p<0.0001$). (C) Survival curves of *Ligase4/Xrcc2/p53* deficient mice. *Lig4,Xrcc2*$^{Nes\text{-}Cre}$ (n=20), *Lig4,Xrcc2*$^{Nes\text{-}Cre}$, p53$^{+/-}$ (n=8), *Lig4,Xrcc2*$^{Nes\text{-}Cre}$, p53$^{-/-}$ (n=3). The survival curves are statistically significantly different ($p<0.0001$). (D) Representative aCGH analysis of chr 11 of *Brca2* and *Lig4,Xrcc2* deficient medulloblastoma associated with *p53* heterozygosity. (E) Summary of genomic rearrangements of chr11 in medulloblastomas of *Brca2*$^{Nes\text{-}Cre}$ and *Lig4/Xrcc2*$^{Nes\text{-}Cre}$. Each column represents a single tumor. Red color indicates that the chromosome exhibit genomic loss.

Figure 2: *Ptch1* is lost in *Brca2, Ligase4, Xrcc2; p53* deficient medulloblastomas.

(A) Representative aCGH analysis of chr13 of *Brca2*, *Lig4*, *Xrcc2* deficient medulloblastomas in *p53* mutant backgrounds. (B) Summary of the genomic rearrangements of chr13 in the medulloblastomas. Each column represents a single tumor, each line represent one chromosome. Each red square indicates that the chromosome exhibit genomic loss. (C) Representative FISH analysis of chr13 showing either deletion or translocation. (D) Sequence analysis of *Ptch1* mRNA from *Lig4*, *Xrcc2*, and *Brca2* deficient medulloblastoma.

Figure 3 : Global gene expression analysis of medulloblastoma. (A) Hierarchical cluster analysis of a selective cohort of genes (from total 319 genes differentially expressed, 46 genes up-regulated/273 genes down-regulated) differentially expressed in the medulloblastomas compared to wildtype (WT) and $p53^{-/-}$ postnatal day 5 and adult (3 month old) cerebellum. The first column shows the address on the MOE 430 A and B gene chips, and the second column shows the GenBank accession numbers. Asterisks indicate multiple hits of the same gene. High (red) to low (blue) expression changes ranging from 0 to 2.5 of normalized values. (B) Quantitative real-time RT-PCR measures the expression level of several signature genes expressed in medulloblastoma to confirm the array analysis.

Figure 4: Genomic analysis of chr 6, 12 and 19 in *Brca2*, *Lig4*, *Xrcc2*, *p53* deficient medulloblastomas. (A) Representative aCGH of chr 6, 12 and 19 in medulloblastomas examined. (B) Representative complete SKY analysis of $Brca2^{Nes\text{-}Cre}$, $p53^{-/-}$. (C) FISH analysis for N-Myc amplification in medulloblastoma. (D) Representative SKY of chr19 showing either deletion or translocation. (E) Summary of the genomic rearrangements of *N-Myc*, *cylin D2*, *Sufu* and *Pten* in the medulloblastomas. Each column represents a single tumor, and each line represents one chromosome. Each red square indicates that the chromosome exhibit genomic loss, each green square indicates that the chromosome presents genomic amplification.

Figure 5: Pten pathway disruption in Brca2/p53 deficient medulloblastoma. (A) Representative medulloblastoma sections showing loss of expression of Pten and up-regulation of levels of phosporylated Akt (P-Akt) and S6 (P-S6) in Brca2/p53 deficient medulloblastoma (Magn.x10 and Magn.x20). (B) Western-blot analysis of Pten, P-S6 and P-

Akt in Brca2/p53 deficient medulloblastoma. (1-3,6: Tumor presenting loss of Pten locus in CGH analysis, 4-5: absence of Pten locus loss in CGH).

Figure 1

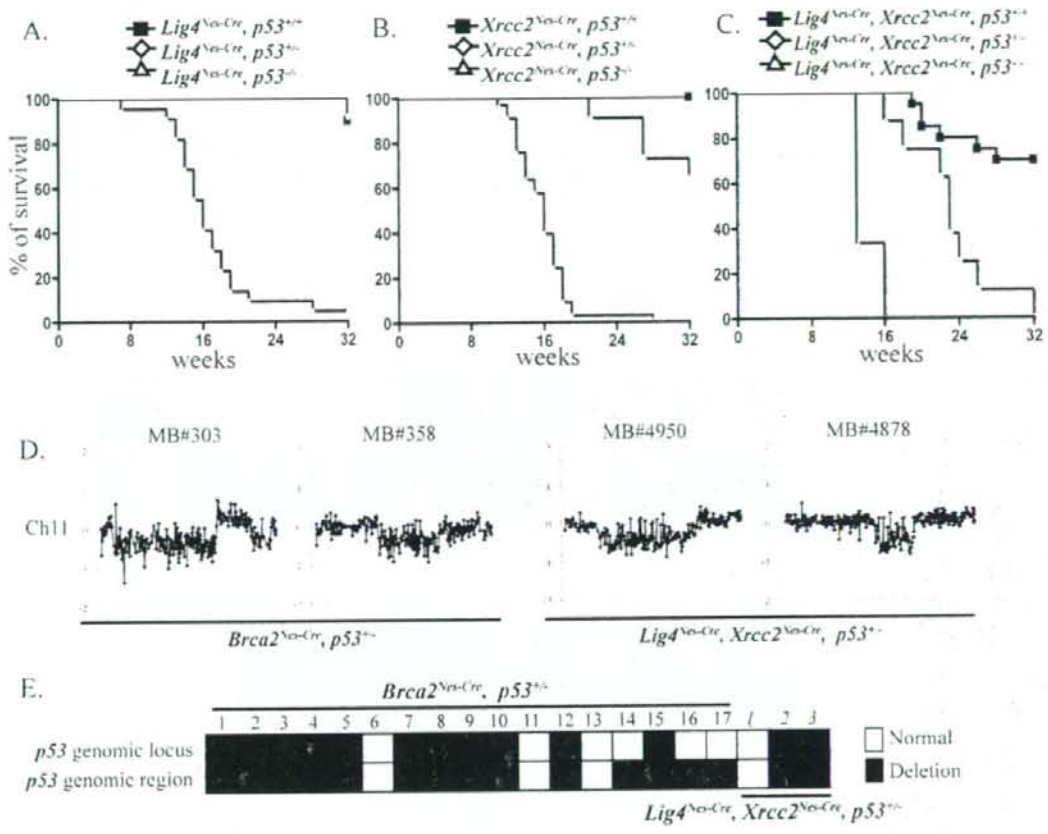
A.
B.
C.
% of survival
weeks
D.
MB#303
MB#358
MB#4950
MB#4878
Ch11
E.
p53 genomic locus
p53 genomic region
Normal
Deletion